NASA Technical Memorandum 100031

Aeroassisted-Vehicle Design Studies for a Manned Mars Mission

G. P. Menees, Ames Research Center, Moffett Field California

October 1987

National Aeronautics and
Space Administration

Ames Research Center
Moffett Field, California 94035

AEROASSISTED-VEHICLE DESIGN STUDIES FOR A MANNED MARS MISSION

Gene P. Menees*
NASA Ames Research Center, Moffett Field, California

Abstract

An aerobrake design that has matured over several years of development accounting for all of the important flow phenomenology which are characteristic of aerobraking vehicles is proposed as the mission baseline. Flight regimes and aerothermal environments for both Mars and Earth entry are calculated using advanced methods to account for real-gas, thermochemical, relaxation effects. The results are correlated with thermal-protection and structural requirements and mission performance capability. The importance of nonequilibrium radiative heating for Earth aerocapture is demonstrated. It is suggested that two aerobrakes of different sizes will produce optimal-performance for the three phases of the mission (i.e., one aerobrake for Mars aerocapture and descent of the surface lander and another for Earth return).

Nomenclature

AOTV = aeroassisted-orbital-transfer-vehicle

c.g. = center of gravity

C_d = drag coefficient

C_m = pitching-moment coefficient

g-load = net of all force vectors on passenger

H = altitude limit of sensible atmosphere

I_{sp} = specific impulse

L/D = lift-to-drag ratio

LEO = low-Earth orbit

m_e = entry mass of vehicle

m_c = mass placed into circular orbit

p_t = total pressure

$\dot{q}_c$ = convective heat flux

$\dot{q}_r$ = nonequilibrium radiative heat flux

Q = stagnation-point total heat load

t = flight time from H = 150 km (Earth) and 100 km (Mars)

V_e = entry velocity

V_x, V_y, V_z = velocity in Cartesian coordinates

x,y,z = Cartesian coordinates from nose

X_{cp}, Y_{cp} = center of pressure coordinates

α = angle of attack

β = ballistic coefficient

ΔV = equivalent propulsive-thrust velocity increment

ρ = atmospheric density

ϕ = meridional angle measured from -y axis

λ = wavelength of radiative heat flux

Introduction

NASA's proposed "Pathfinder" initiative for future exploration of the solar system includes plans for a sample return mission from Mars. This is probably the most ambitious planetary program to date. The initial phase could probably be an unmanned mission that is the forerunner to manned exploration of Mars. Consequently, large payload capability in orbit, on the surface, and for return to Earth is of high priority, because a variety of samples from different regions of the planet are required for completeness of the geographical survey.

A key factor in the mission feasibility analysis is the use of aerobraking rather than retropropulsion to achieve the deceleration for orbit modification at Mars, as well as, Earth. The crucial issue of the aerocapture approach is whether the benefit of reduced fuel mass more than compensates for the added weight penalties resulting from the aeroassist apparatus and thermal-protection-system (TPS) required to accommodate atmospheric braking and heating.

The basic principles of aerobraking have been demonstrated in feasibility studies dating back more than a generation. An excellent review is given in Ref. 1. The theoretical concept is to

*Research Scientist. Associate Fellow AIAA. Associate Editor AIAA Journal of Spacecraft and Rockets.

achieve a new orbital state by dissipating a spacecraft's orbital energy during grazing passes through a planet's upper atmosphere. Except for descents (e.g., the Apollo and Fire projects), aerobraking to a new orbit has never been attempted in actual flight tests because of the belief that the undertaking was beyond the capability of available technology. With the rapid advancements in the enabling technology of adaptive guidance logic in the past decade, aerobraking is now considered promising as a useful technology for space missions.

The present study examines the application of aerobraking to the Mars sample return mission based on a wealth of experience gained at the NASA Ames Research Center in aeroassisted-vehicle research for Earth-Moon space[2-5] and the Titan aerocapture mission.[6] The manned-scenario is analyzed herein because of the greater technology challenge, which will probably satisfy all other mission requirements.

The focus of this study is the aerobrake vehicle design[5] proposed by NASA Ames Research Center for the AOTV fleet. This design has been under extensive development for several years in support of the space station program and has reached considerable maturity. It incorporates many advanced features that were the first to account for the major flow phenomena that are characteristic of an aerobrake vehicle. Moreover, it has served as the baseline for other current leading aerobrake designs.

The effects of Mars' unique atmospheric composition (95% CO_2, 4% N_2, 1% Argon) and low density on the aerothermodynamic environment and heat-shield response is analyzed using state-of-the-art codes developed at NASA Ames that incorporate real-gas thermochemical relaxation effects. This capability is also necessary for the Earth-return mission because of the high superorbital entry velocities which cause severe real-gas effects that are crucial to surface heating and thermal-protection requirements. Trade-off studies are made that contrast the range of entry velocities of interest for Mars and Earth and the various Earth return modes (direct, aerocapture, all-propulsive). The results are correlated with sizing and weight penalty requirements for the aerobrake and the impact on performance capability determined for the complete mission (i.e., Mars and Earth aerocapture; Mars surface landing).

Vehicle Design

Complete details of the aerobrake design and resulting aerodynamic/aerothermodynamic performance are given in Ref. 5. A brief summary of major features relevant to this study are given below.

Geometry

The basic configuration is illustrated in Fig. 1 and consists of a raked-off, spherically-blunted, circular cone. The design is generated in parametric optimization studies from a generalized biconic geometry code, which computes the body coordinates for variable cone angle, rake angle, and nose radius. The integration of the vehicle systems components (engines, fuel tanks, command/control module, cargo bay) into the overall configuration is shown in Fig. 2. The arrangement and size were carefully analyzed to provide several major improvements over other leading proposals. These include: 1) maintain longitudinal stability with shifting center of gravity resulting from propellant consumption and variable payload; 2) prevent flow impingement on afterbody components by providing sufficient base-flow clearance angle (thus avoiding high concentrated heat fluxes and resultant thermal-protection weight penalties); 3) rounding the frustrum to alleviate highly concentrated edge heat fluxes. Although the current design was sized for the Lunar-return mission, it can be readily modified to accommodate superorbital entry velocities.

Aerodynamic Characteristics

The lift, drag, and pitching-moment characteristics were determined from Newtonian hypersonic flow theory. Although this approach is a reasonable approximation for lift and drag, considerable uncertainty can result for the stability predictions because of the effects of viscous and real gas phenomena. This problem will be alleviated in the future, since computational-fluid-dynamic codes that account for all relevant physics are under development at NASA and other locations. However, for the present study, the uncertainties are not a major concern because all leading aerobraking designs have been analyzed on the same analytical basis and our intent is to focus attention on the best design. The predicted aerodynamic characteristics are given in Fig. 3. Values of L/D range from about 0.34 to 0.1 over an α range of -10° to +10° (Fig. 3(a)), with attendant pitching stability (Fig. 3(b)). The insert in Fig. 3(b) illustrates the resultant force lines for each α and the location where they converge (metacenter). The restoring moment occurs between the metacenter and center of gravity. Consequently, it is beneficial to have a large distance between the metacenter and aerobrake surface, since the metacenter is the theoretical limit for downstream location of the center of gravity.

Trajectory Program

The research tool used in this paper is our long-used computer program WTRAJ, which was developed at Ames Research Center by J. F. Wilson. This program is straightforward, fast, and

accurate for our purposes. Its focus is near planet trajectories, including orbits outside the atmosphere and atmospheric aerotransits. The program numerically integrates Newton's equations of motion. A predictor-corrector numerical scheme is used, and time is the independent variable. The geometry is fully three-dimensional with rotating planet (the atmosphere's rotational speed is a function of latitude). The integration proceeds in the inertial coordinate system. The vehicle's state vector is at all times calculated in both inertial coordinates (x, y, z, V_x, V_y, V_z) and astrodynamic coordinates (radius, latitude, longitude, speed, flight angle, azimuth). The air-relative speed is also calculated, and all orbital elements (semimajor length, eccentricity, inclination, longitude of ascending node, longitude of periapsis, true anomaly) are also calculated at all times. The program can account for those perturbations caused by the planet's oblateness and by a single moon; however, since the trajectories of this study are at low altitude and of short duration, these perturbations are neglected here. The aerodynamic forces of drag and lift are included in the program; the direction of the lift vector may be changed to produce a lateral (turning) force; also, the roll may be controlled (automatically) to produce a glide trajectory (constant flight angle). The reference atmosphere models are tables of density versus altitude, which for Earth is based on the 1962 U. S. Standard Atmosphere and for Mars on the Viking fly-by data. The thrust force is also included in the code. The vehicle's mass decreases at a rate predetermined by the specific impulse of the rocket engine, and at each computational time interval, the stagnation-point heating rate and net of all force vectors felt by the passenger (the g-load) are calculated.

Mars Aerocapture

All calculations are based on the reference atmospheric density-altitude variations shown in Fig. 4. The Mars data was obtained from Viking fly-by measurements and presented by Kliore.[7] Results for all-aerocapture transatmospheric maneuvers to a circular orbit at 200 km altitude are given in Figs. 5-8.

Typical flight trajectories are shown in Fig. 5 for a nominal V_e of 6.5 km/sec and two values of β (805 and 201 kg/m^2). Results are shown only for single passes, since exploratory analysis showed that the first of multiple passes must reduce the flight velocity below the hyperbolic value to achieve orbital closure. The βs are based on m_e = 134.5 Mg, which was estimated from previous mission analysis studies[8] to provide an Earth-return m_e of 5 Mg (approximately that required for the manned mission). The basic reference area for the βs corresponds to a 6 m-radius aerobrake (β = 805 kg/m^2) and was calculated for Lunar-return missions with detailed analysis of the thermal-protection and structural requirements.[3,6] Consequently, it serves as the sizing basis for all other applications. The other value of β (201 kg/m^2) was obtained by doubling the basic radius to a value of 12 m and results in a significant effect on the flight duration and perigee location. These results were obtained for L/D = -01. This is the recommended value, estimated from previous work,[3] to provide a sufficient safety margin for the aerobrake's lifting capability to accommodate unpredictable variations in the atmospheric structure resulting from daily, seasonal, and solar temperature effects. The maximum L/D is seen to be about ±0.3 in Fig. 3. A margin of ±0.2 was considered necessary to handle the density dispersions in the Earth's upper atmosphere (especially the pot-hole density phenomena measured in Shuttle flights). Although the variations in Mars' upper atmosphere will differ from that of Earth, some strong variations are known to occur.[7] Consequently, a conservative analysis was considered best with the previous work used as the baseline.

The distributions over the flight trajectories of $\dot{q}_c$ and the g-loads are presented in Figs. 6(a) and 6(b), respectively. The significance of these two critical design parameters to the aerobrake sizing estimates will be discussed in a following section (Mass Efficiency). Analysis has shown that no significant thermochemical relaxation effects on heating and pressure occur for Mars entry. However, there may possibly be some mild vibrational-nonequilibrium effects because of the triatomic structure of the carbon-dioxide molecule. In addition, surface catalysis effects in a carbon-dioxide environment are not known. These two issues are currently being studied at NASA Ames. Fully-catalytic heating predictions are given in Fig. 6 for conservatism.

Since the L/D safety margin is still somewhat of an open issue, calculations were made to determine the potential benefits of flying the vehicle at greater values of negative lift. The results are summarized in Fig. 7 for several key design parameters. These are the minimum H (or perigee of the flight trajectory) and maximum $\dot{q}_c$, g-load, and p_t shown in Figs. 7(a) thru 7(d), respectively. The benefits of negative L/D and detriments of positive L/D are evident. Significant reductions in surface heating, surface pressures, and g-loads are obtained if, for example, flying at L/D = -0.2 is demonstrated to be possible. This would greatly enhance mission performance capability.

The effects of V_e over the range of values considered for Mars entry are shown in Fig. 8. Results are given for three values of β (805, 201, and 89.4 kg/m^2), which correspond to the baseline 6 m-radius aerobrake with double and triple this value, respectively. The effect of β in controlling the magnitudes and rate of increase of $\dot{q}_c$, g-load, and p_t is dramatic. The results indicate that the aerobrake can be sized without difficulty with prudent selection

of V_e and β to achieve acceptable weight penalties. This issue will be addressed in greater detail in a subsequent section (Mass Efficiency).

It is also suggested that the Mars aerobrake may serve the dual role of providing the descent capability for the surface lander, as well as, capture to a closed orbit. The results of the previous mission analysis study[8] show that the descent heating and total pressure data are much less severe than for Mars capture, but the pressure substantially exceeds that for Earth capture. Consequently, the aerobrake may possibly be used for descent if it can be shown that dismounting from the orbiter and attachment to the lander is feasible.

Earth Aerocapture

Calculations were made using the 1962 U. S. Standard Atmosphere. Flight trajectories that contrast Mars return modes with direct entry and aerocapture involving single and double passes to orbital rendezvous at 400 km altitude are given in Fig. 9. These results were obtained for a favorable return V_e of 13 km/sec, L/D = -0.1, and β = 29 kg/m^2. This corresponds to m_e = 5 Mg with an aerobrake radius of 6 m, which was established previously for the Lunar return mission and is used as the baseline herein because of its mature development.

The potential benefits of aerocapture, as shown by ΔV, are illustrated in Fig. 10. The equivalent ΔV, which is an indicator of propellant weight penalties, is compared for the all-propulsive and aerocapture maneuvers. The values for the single and double pass aerocapture cases are trivial relative to that for the all-propulsive case, which is about 5.4 km/sec. Even for the most advanced rocket engines being developed for orbital-transfer vehicles (e.g., category IV of the various RL-10 derivatives having a specific impulse of 480 sec), this represents about 70% of the vehicle mass in propellant usage and would probably make the mission impossible. In addition, Fig. 10 illustrates that the double pass mode has trivial advantages over single passes, as mentioned previously (Mars Aerocapture). This probably applies generally to multiple pass scenarios, unless they are also combined with propulsive capability. This result could possibly have important consequences to the contamination issue, since, as shown in Fig. 11, the duration of even two passes exceeds that of a single pass by a factor of twenty and contributes to the probability of a catastrophic failure.

The predicted stagnation-point aerothermodynamic heating characteristics (the maximum surface values) are given in Fig. 12. The convective heat flux distributions (Fig. 12(a)) are finite-rate values that assume a wall catalytic efficiency similar to that of the Shuttle-type ceramic materials. These are appropriate for the flexible-ceramic cloths under development for aerobrake surfaces operating near Earth. The importance of finite-rate, thermochemical effects for the rarefied, hypervelocity, high-altitude flight regimes and large-scale bodies of interest herein is demonstrated by the nonequilibrium radiative heating distributions shown in Fig. 12(b). These rates are equivalent in magnitude to the convective heating. The nonequilibrium results were determined from the work of Park,[9] who recognized this phenomenon for Earth entry. Unlike the convective heating, however, which must be absorbed, the radiative heating may be substantially reduced by proper design of the aerobrake material's optical properties. For example, it has been shown that ceramic thermal-protection materials can be tailored to reflect incident radiation while efficiently reradiating convective heat flux. The intensity of the incident radiative flux of high-temperature air is strongest in the short wavelengths of the visible range (i.e., $\lambda < 2$ μm), where reflectivity is highest for these materials. Conversely, by Kirchoff's law, the emissivity is highest in the longer wavelengths of the infrared (i.e., $\lambda > 2$ μm), where the surface emission is greatest. This occurs because the source of the incident flux is always at much higher temperatures (>10,000 K) than that of the aerobrake surface (<1000 K). As a result, the spectral optical properties are nearly matched to the thermal environment.

The total heat loads resulting from the combined convective and radiative heat fluxes for a typical reflectivity of 80% for a candidate surface material are given in Fig. 13. In addition, the g-load distributions are shown in Fig. 14 for the single-pass case of trajectory B.

The effects of L/D on perigee location and maximum $\dot{q}_c$, g-load, and p_t are given in Fig. 15 for trajectory B and V_e = 13 km/sec. As shown previously for Mars aerocapture, the benefits of flying at greater negative lift are substantial in reducing the key aerobrake sizing parameters ($\dot{q}_c + \dot{q}_r$, g-load, and p_t). However, this possibility for Earth is unlikely as shown in previous work,[3] where a L/D margin of ±0.2 was required to accommodate the unpredictable atmospheric density dispersions. The effects of V_e at L/D = -0.1 are shown in Fig. 16 for the same flight parameters. These results will be correlated with aerobrake sizing estimates in the following section.

Mass Efficiency

To determine the mass efficiency or savings in propellant mass provided by the aerocapture maneuvers, estimates must be made of the mass penalty resulting from the aerobrake and associated thermal-protection requirements. The baseline 6 m-radius aerobrake[5] was selected for this study because it had received detailed analysis and good estimates of the associated mass penalty

were available to guide other sizing exercises. The baseline design criteria consisted of a maximum surface heat flux of 23 W/cm^2 to remain within Shuttle TPS capability, a g-load of the order of two, and a total pressure of 1750 N/m^2. The aerobrake mass penalty for these conditions was about 15% of the entry mass of 5 Mg for lunar return.

Considering the relative trades in the sizing parameters for Mars and Earth aerocapture shown in Figs. 8 and 16, respectively, some recommendations can be made concerning aerobrake sizing. First, the baseline size is probably adequate for Earth entry at a maximum V_e of 11.5 km/sec, which corresponds to the previous mission analysis studies.[8] The sizing parameters are slightly higher than the baseline for this case [i.e., $\dot{q}_c + \dot{q}_r = 26$ W/cm^2 (21 W/cm^2 convective + 5 W/cm^2 radiative assuming the surface reflectivity is 80%), g-load = 3.5, and $p_t = 1900$ N/m^2]; however, the agreement is acceptable within engineering accuracy. In addition, the aerobrake can be strengthened somewhat by adding insulation and structural integrity, so that the mass penalty is increased to a total of 20% to accommodate deficiencies.

For the Mars aerocapture case, the results shown in Fig. 8 indicate that the baseline aerobrake size ($\beta = 805$ kg/m^2) is out of the question for most of the V_e range, because of the very high values of p_t, which exceed 2×10^4 N/m^2. Decreasing β, however, dramatically reduces p_t to acceptable levels. For example, $\beta = 201$ kg/m^2 corresponds to a two-fold increase in the aerobrake radius to 12 m, which increases the mass by a factor of four. For a reasonable V_e value of 6 km/sec, the p_t exceeds the baseline case by about a factor of 3.4. The $\dot{q}_c$ and g-load are, however, well within acceptable limits. The combination of β and p_t increase the aerobrake mass penalty by a factor of 13.4 or 200% over the baseline, which corresponds to a total penalty of 10^4 kg. In addition, there will be flow-impingement on the vehicle afterbody because the Mars m_e is about a factor of 27 greater than that for Earth, and the increased aerobrake radius provides protection for only an eight-fold increase. Consequently, some shielding technique will be required to protect a substantial portion of the vehicle's afterbody. It is difficult to estimate the necessary mass penalty. Based on the previous work with deployable aluminum panels,[3-5] a total penalty of 10% of the entry mass (134.5 Mg) seems reasonable.

An alternate approach to achieving the same result is to triple the aerobrake radius to 18 m ($\beta = 81.4$ kg/m^2), which provides a ninefold increase in the mass penalty. The p_t is only about 10% greater than the baseline for this case, while the $\dot{q}_c$ and g-load are very low. Consequently, a total mass penalty of about 10% is again obtained (as for the $\beta = 201$ case). The big advantage of the $\beta = 81.4$ case, however, is that the cargo volume is increased by a factor of 27 to agree with the requirement resulting from the ratio of Mars to Earth entry masses. This sizes the aerobrake geometry correctly to prevent flow impingement and avoids many technical heat-shielding issues in the wakeflow. The major consideration, however, is that the aerobrake is now 36 m (about 100 ft) in diameter and may be too big and cumbersome to package or handle effectively.

The mass efficiency factors for the all-propulsive and aerocapture maneuvers including the estimated penalties for the aerobrake are compared in Fig. 17. The aerocapture results were determined assuming the vehicle decelerates propulsively from the designated V_e to the acceptable entry values discussed above (i.e., 6 km/sec for Mars and 11.5 km/sec for Earth). The shaded areas with these limitations then represent the actual propellant mass savings that may be allocated to other cargo. For Mars, this factor ranges from about 30% to 15% as V_e varies from 6 to 8 km/sec and for Earth from 33% to 7% for the V_e range of 11.5 to 15 km/sec. The savings are substantial, even within the restrictions of current materials technology, and can be expected to be extended because of normal-growth technology and the long time frame involved to proposed mission launch dates (i.e., circa the year 2000).

Concluding Remarks

The results of this preliminary, exploratory study indicate that the benefits of aerocapture are so great that it could be the key enabling technology for the manned Mars Mission. In essentially its original form, the near-Earth version of a proposed baseline aerobrake design (i.e., 6 m radius) is adequate for the Earth-capture phase of the mission. The importance of non-equilibrium radiative heating for Earth entry was demonstrated. With proper sizing (i.e., either a factor of two or three greater than the near-Earth version), the same design is qualified for Mars capture and possibly the descent of the surface lander. Consequently, two aerobrakes may be appropriate for the three aerobraking elements of the mission. Even accounting for the mass penalty resulting from the aerobrake and associated thermal-protection requirements, the propellant mass savings is at least 30% of the entry mass for both Mars and Earth capture. This is especially significant for Mars because of the large entry mass. Developing normal-growth technology for rocket engines and thermal-protection materials can be expected to enhance the benefits of aerocapture because of the long time scale before proposed launch dates (i.e., circa the turn of the century).

Future work to refine the aerocapture requirements will include a detailed analysis of the weight trades resulting from interplanetary transit of various aerobrake options. This involves, for example, determining the number of aerobrakes that will actually accommodate the

three major elements of the mission. In addition, an examination of possible abort mode scenarios will be undertaken because of sample contamination concerns of Earth's environment.

References

[1]Wallberg, G. D., "A Survey of Aeroassisted Orbit Transfer." AIAA Journal of Spacecraft and Rockets, Vol. 22, No. 2, March-April, 1985, pp. 104-111.

[2]Menees, G. P., "Thermal Protection Requirements for Near-Earth Aeroassisted Orbital Transfer Vehicle Missions." Progress in Astronautics and Aeronautics: Thermal Design of Aeroassisted Orbital Transfer Vehicles, Vol. 96, edited by H. F. Nelson, 1985, pp. 257-285.

[3]Menees, G. P., Park, C., and Wilson, J. F., "Design and Performance Analysis of a Conical Aerobrake Orbital Transfer Vehicle Concept." Progress in Astronautics and Aeronautics: Thermal Design of Aeroassisted Orbital Transfer Vehicles, Vol. 96, edited by H. F. Nelson, 1985, pp. 286-308.

[4]Menees, G. P., Davies, C. B., Wilson, J. F., and Brown, K. G., "Aerothermodynamic Heating Analysis of Aerobraking and Aeromaneuvering Orbital Transfer Vehicles." Progress in Astronautics and Aeronautics: Thermal Design of Aeroassisted Orbital Transfer Vehicles, Vol. 96, edited by H. F. Nelson, 1985, pp. 338-360.

[5]Davies, C. B. and Park, C., "Aerodynamic and Thermal Characteristics of a Modified Raked-Off Blunted Cone." AIAA Paper 86-1309, AIAA/ASME 4th Joint Thermophysics and Heat Transfer Conference, Boston, MA, June 2-4, 1986.

[6]Menees, G. P., "Trajectory Analysis of Radiative Heating for Planetary Missions with Aerobraking of Spacecraft." AIAA Journal of Spacecraft and Rockets, Vol. 22, 1985, pp. 37-45.

[7]The Mars Reference Atmosphere, edited by A. Kliore, 1st ed., Oxford, Committee on Space Research by Pergamon Press, 1982.

[8]Manned Mars Missions - A Working Group Report, Vol. I, edited by M. B. Duke and P. W. Keaton, published by NASA and Los Alamos. Based on papers presented at: Marshall Space Flight Center, Huntsville, Alabama, June 10-14, 1985.

[9]Park, C., "Calculation of Nonequilibrium Radiation in the Flight Regimes of Aeroassisted Orbital Transfer Vehicles." Progress in Astronautics and Aeronautics: Thermal Design of Aeroassisted Orbital Transfer Vehicle, Vol. 96, edited by H. F. Nelson, 1985, pp. 395-418.

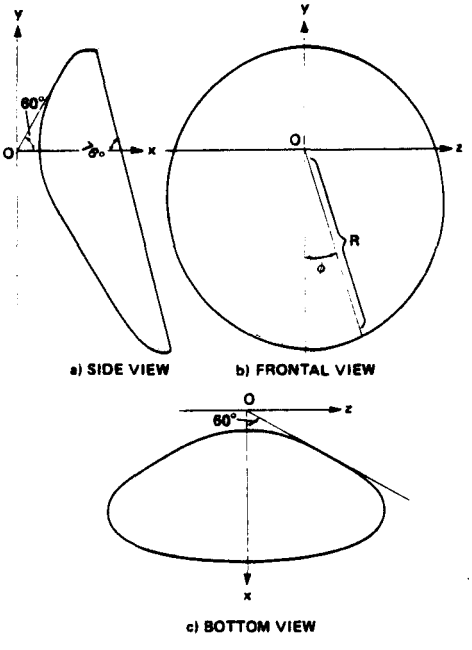

Fig. 1 Baseline spherically-blunted, raked-off sphere-cone aerobrake geometry (Ref. 5).

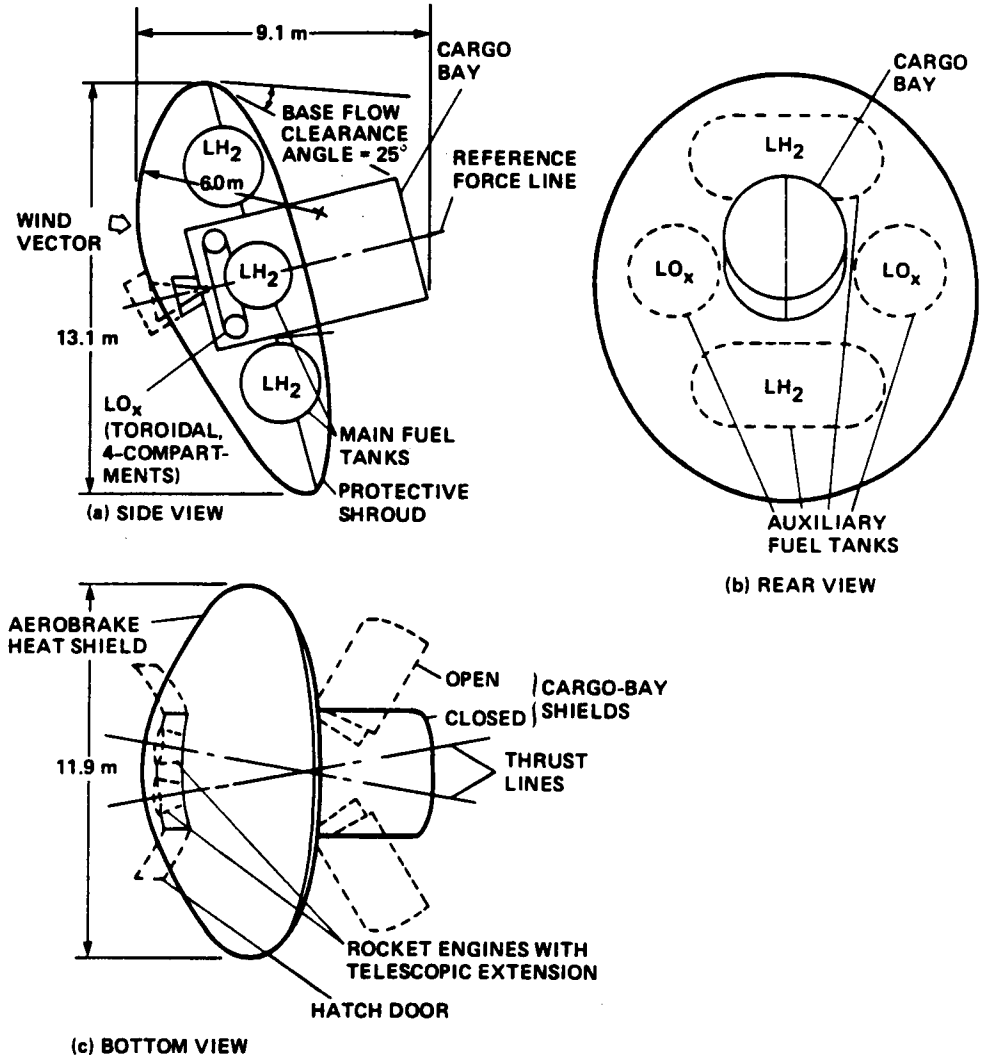

Fig. 2 Arrangement of vehicle systems components sized for Lunar-return mission (Ref. 5).

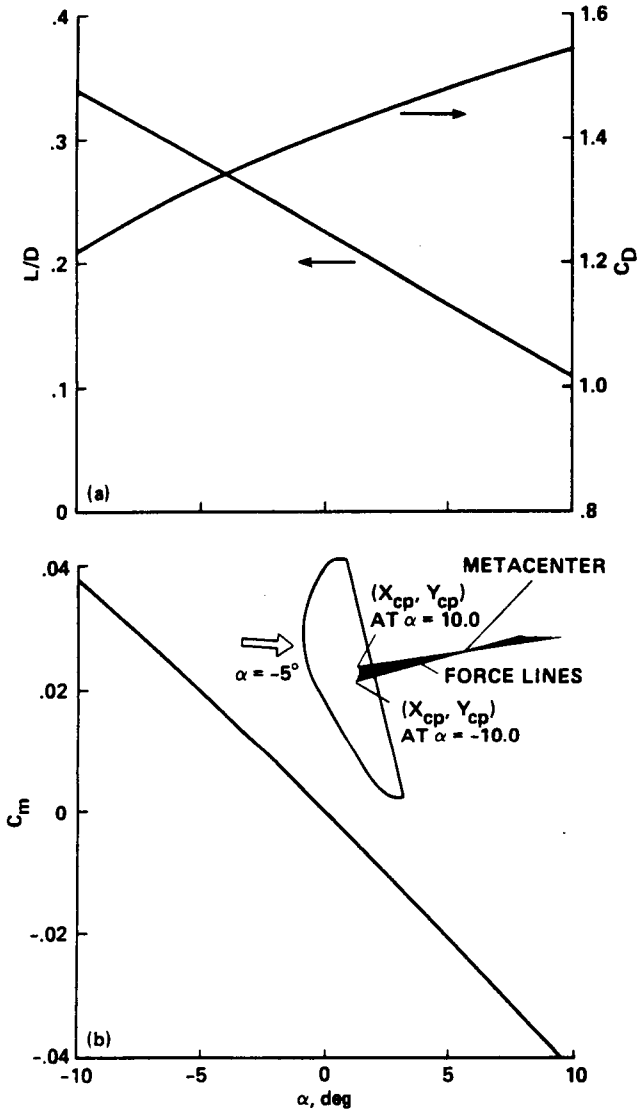

Fig. 3 Aerodynamic characteristics: a) lift and drag; b) longitudinal stability (Ref. 5).

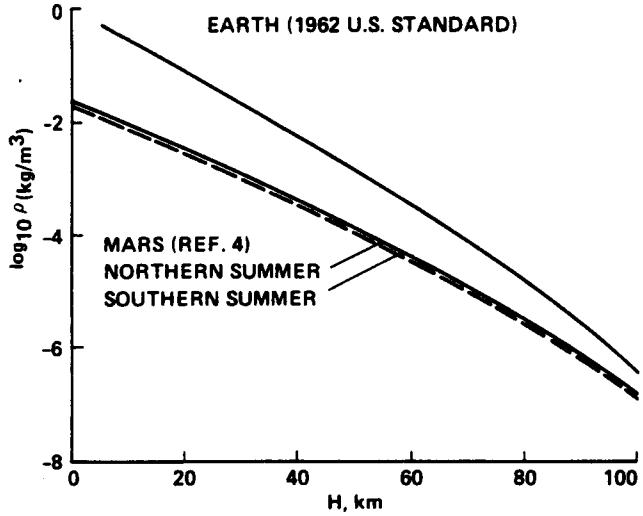

Fig. 4 Comparison of reference atmospheres for Mars and Earth.

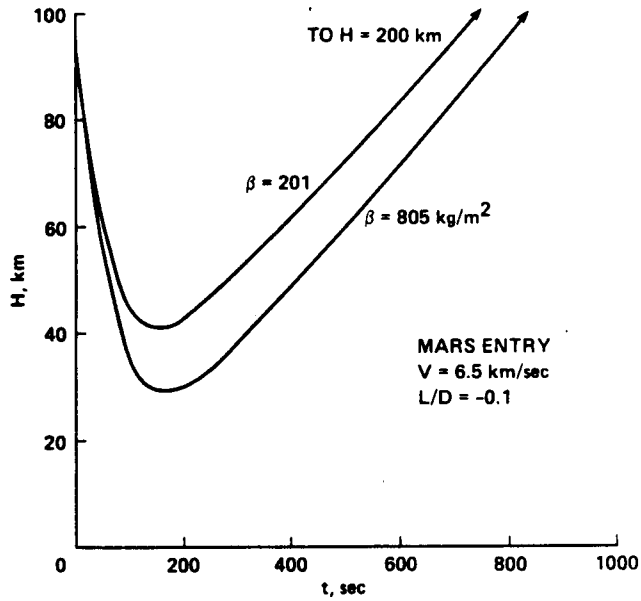

Fig. 5 Mars transatmospheric flight trajectories for aerocapture to LEO at 200 km altitude.

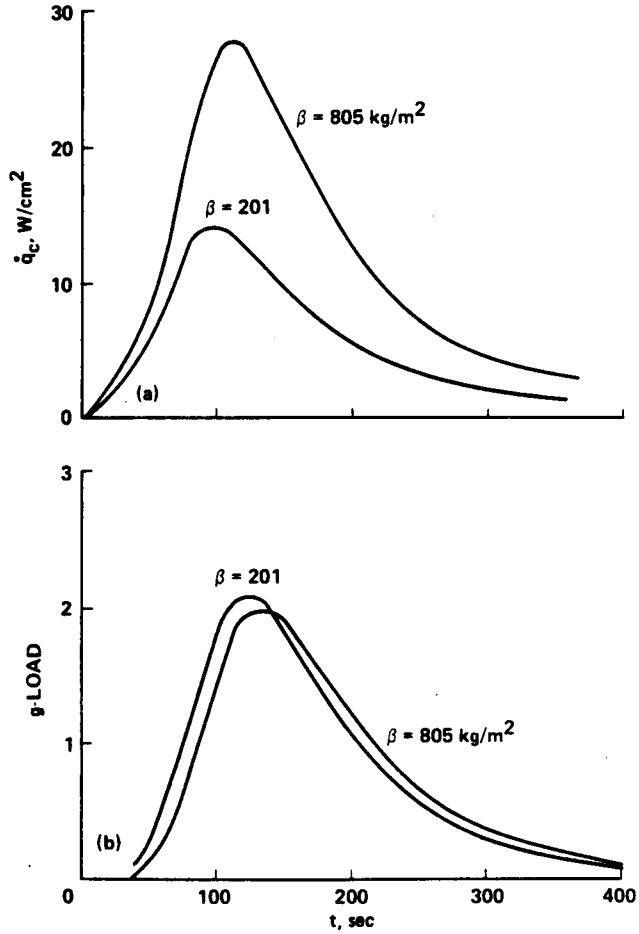

Fig. 6 Mars entry characteristics for V_e = 6.5 km/sec and L/D = -0.1: a) stagnation-point fully-catalytic heating; b) g-loads.

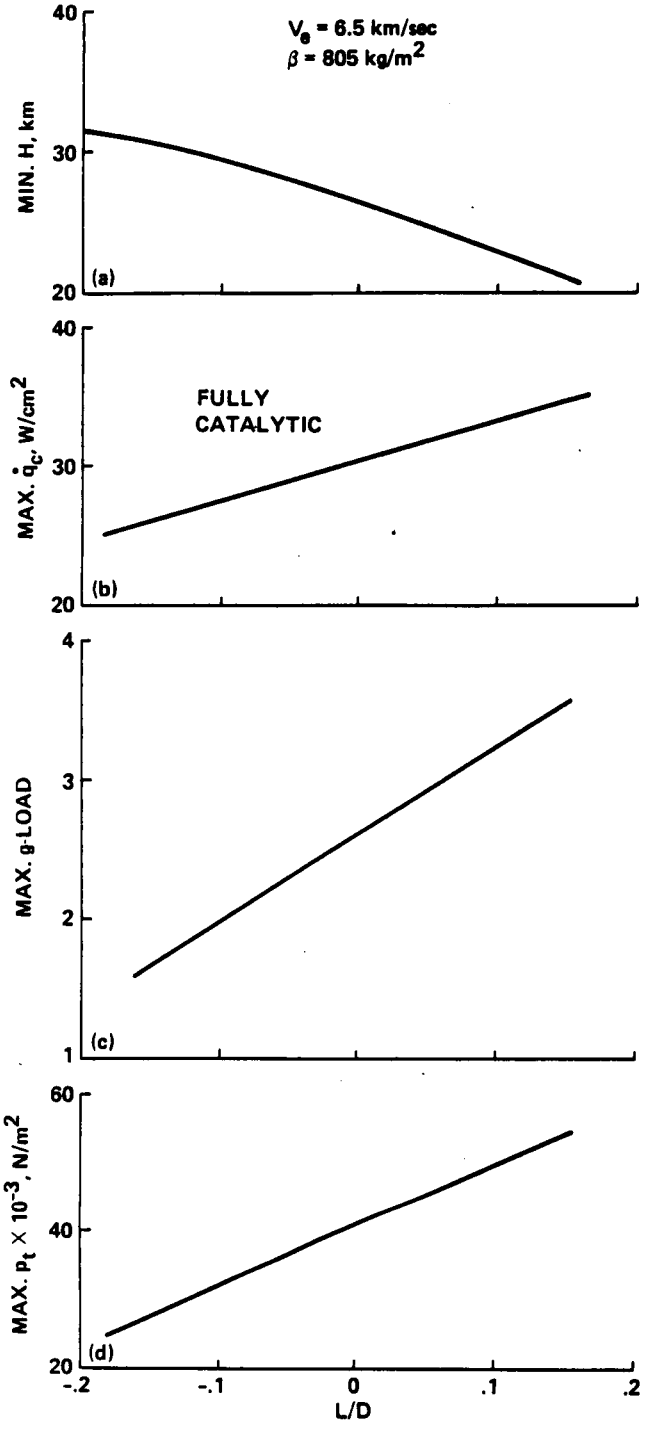

Fig. 7 Mars L/D effects at V_e = 6.5 km/sec: a) minimum altitude; b) maximum heating; c) maximum g-load; d) maximum total pressure.

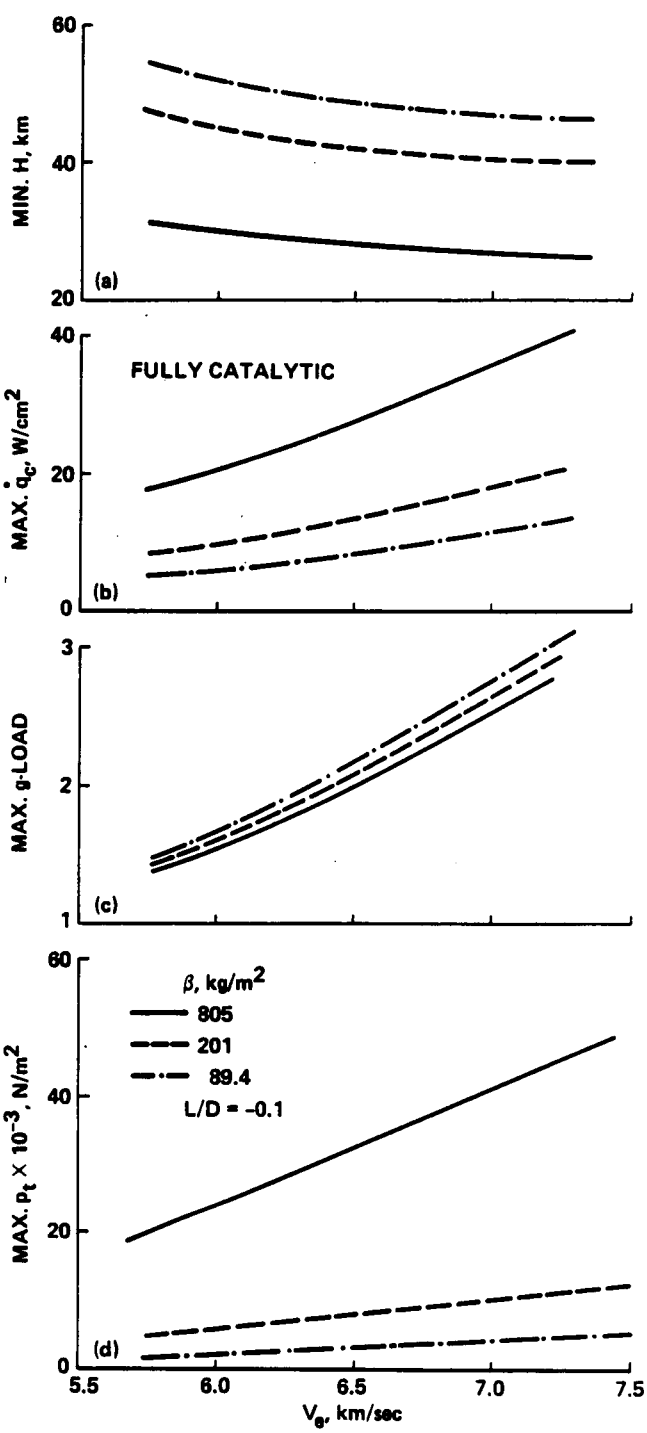

Fig. 8 Mars V_e effects at L/D = -0.1: a) minimum altitude; b) maximum heating; c) maximum g-load; d) maximum total pressure.

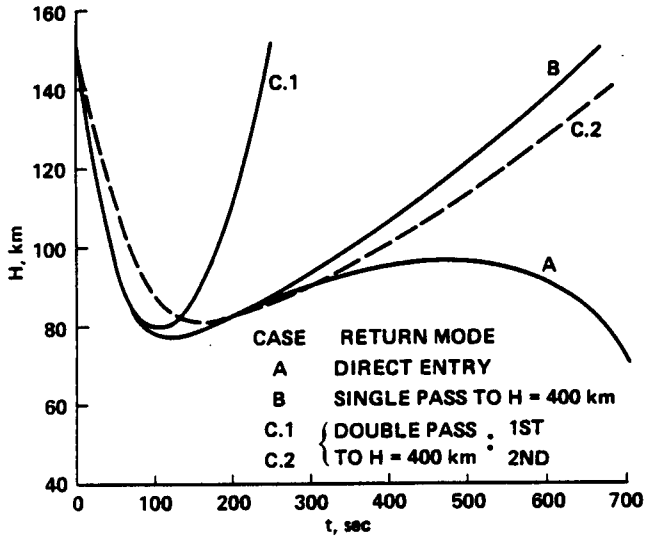

Fig. 9 Transatmospheric flight trajectories for Earth aerocapture modes to LEO at H = 400 km (V_e = 13 km/sec, β = 29 kg/m^2, L/D = -0.1).

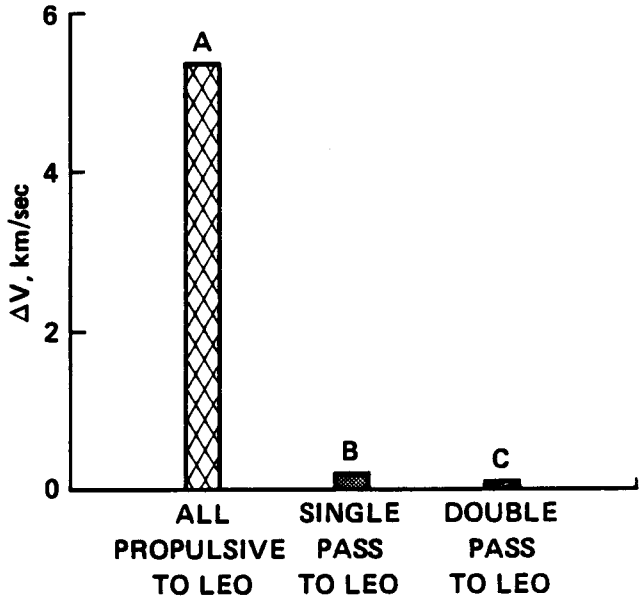

Fig. 10 Equivalent propulsive thrust velocity increment (ΔV) for circularization at LEO.

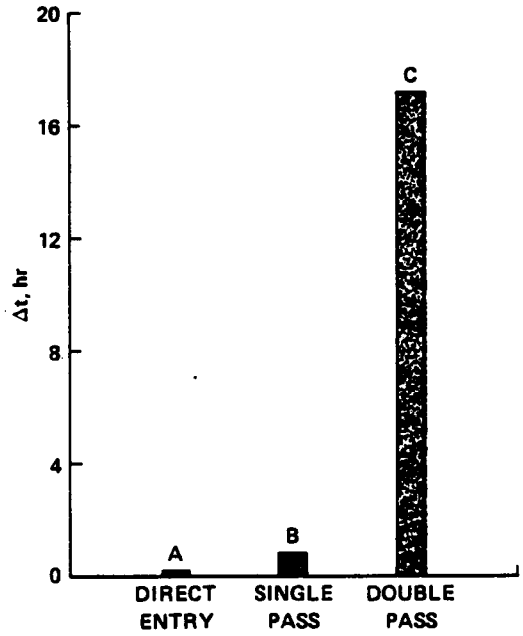

Fig. 11 Relative time interval (Δt) for completion of various Earth aerocapture modes.

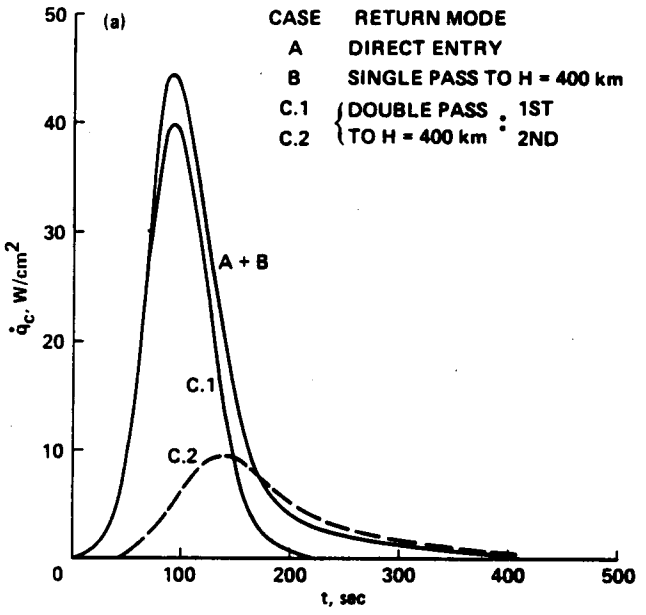

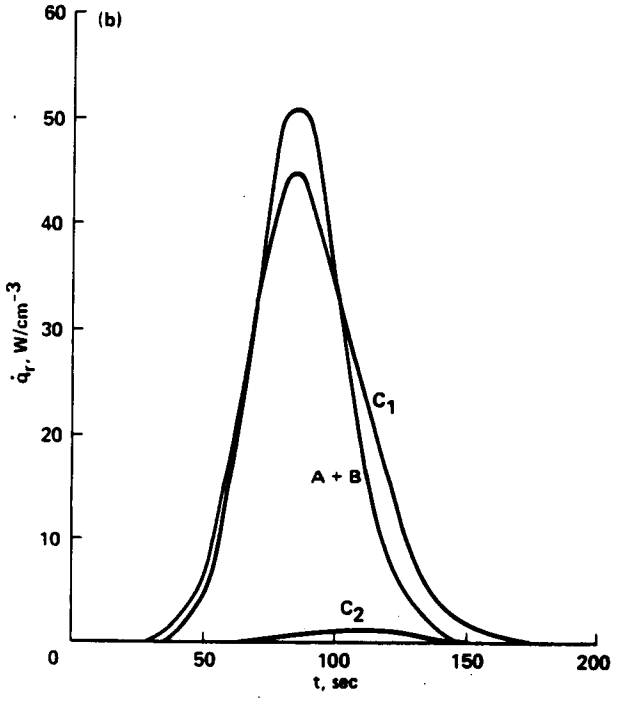

Fig. 12 Stagnation-point heat-flux distribution for trajectory B: a) finite-rate catalytic convective; b) nonequilibrium radiative.

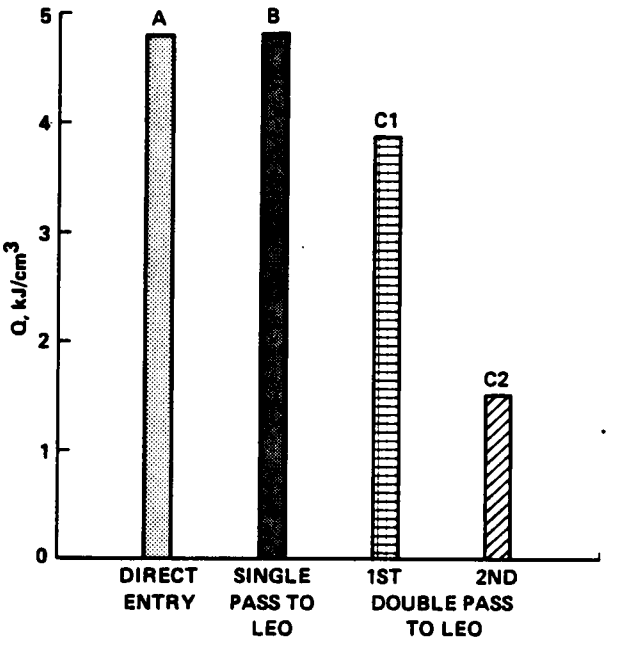

Fig. 13 Total heat loads (Q) over transatmospheric flight trajectories for various Earth aerocapture modes.

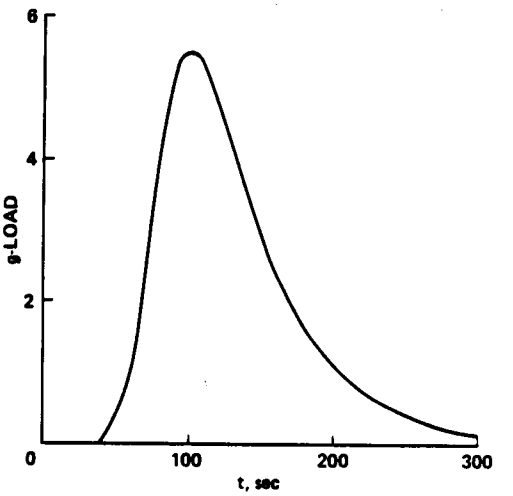

Fig. 14 g-load distributions for trajectory B.

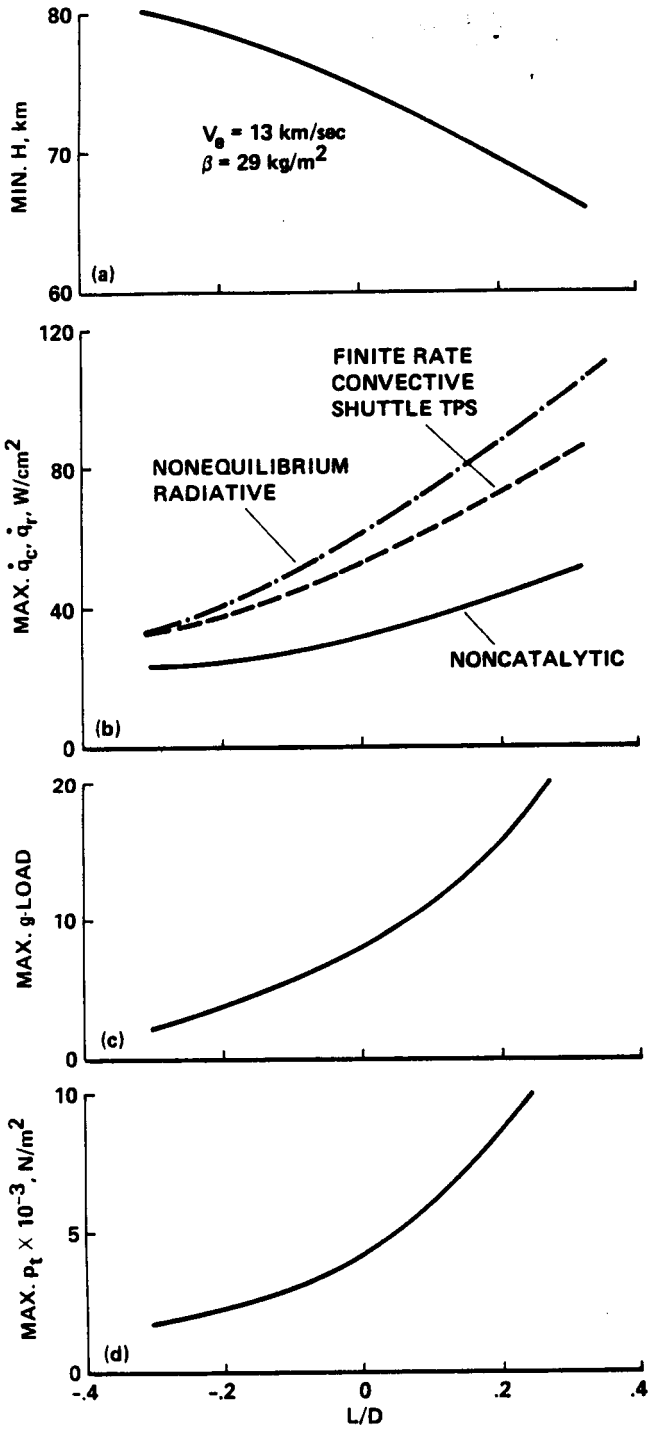

Fig. 15 Earth L/D effects at V_e = 13 km/sec: a) minimum altitude; b) maximum heating; c) maximum g-load; d) maximum total pressure.

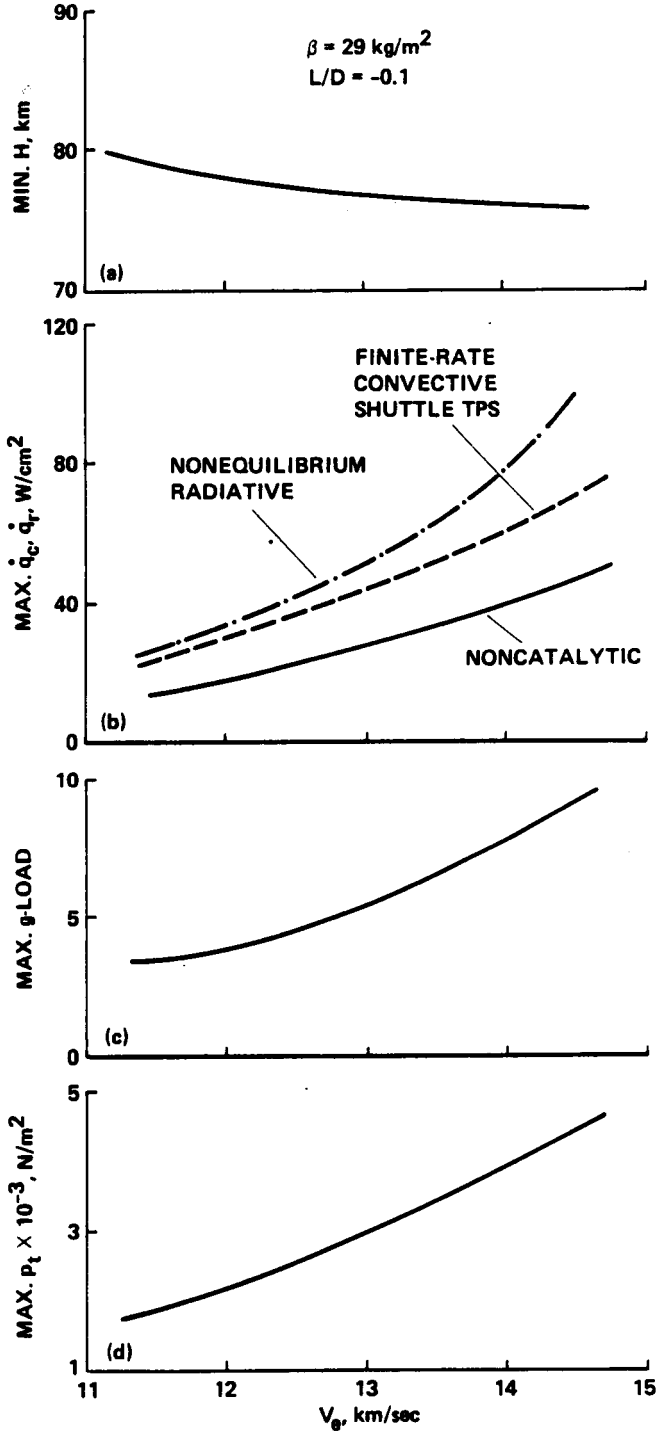

Fig. 16 Earth V_e effects for L/D = -0.1: a) minimum altitude; b) maximum heating; c) maximum g-load; d) maximum total pressure.

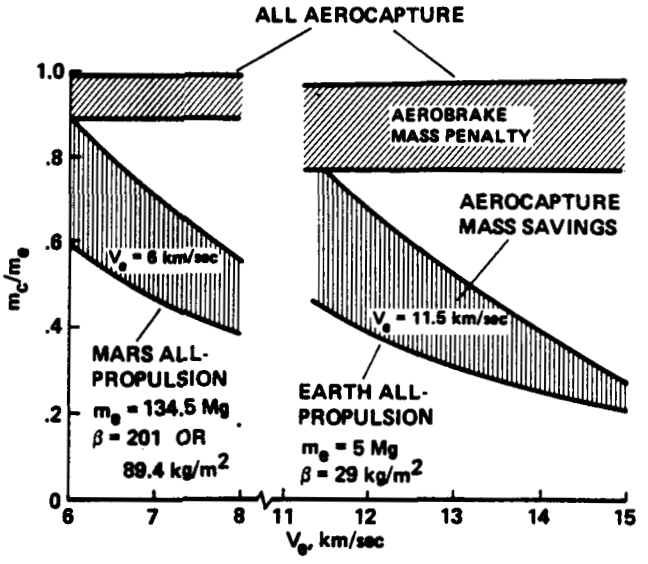

Fig. 17 Mass efficiency factors for Mars and Earth aerocapture showing potential propellant savings for L/D = -0.1.

NASA
National Aeronautics and Space Administration

Report Documentation Page

1. Report No.	2. Government Accession No.	3. Recipient's Catalog No.
NASA TM-100031		

4. Title and Subtitle

Aeroassisted-Vehicle Design Studies for a Manned Mars Mission

5. Report Date

October 1987

6. Performing Organization Code

7. Author(s)

Gene P. Menees

8. Performing Organization Report No.

A-87356

10. Work Unit No.

505-404-1

9. Performing Organization Name and Address

Ames Research Center
Moffett Field, CA 94035-5000

11. Contract or Grant No.

13. Type of Report and Period Covered

Technical Memorandum

12. Sponsoring Agency Name and Address

National Aeronautics and Space Administration
Washington, DC 20546-0001

14. Sponsoring Agency Code

15. Supplementary Notes

Point of Contact: Gene P. Menees, Ames Research Center, M/S 230-2, Moffett Field, CA 94035-5000 (415) 694-6086 or FTS 464-6086

16. Abstract

An aerobrake design that has matured over several years of development accounting for all of the important flow phenomenology which are characteristic of aerobraking vehicles is proposed as the mission baseline. Flight regimes and aerothermal environments for both Mars and Earth entry are calculated using advanced methods to account for real-gas, thermochemical, relaxation effects. The results are correlated with thermal-protection and structural requirements and mission performance capability. The importance of non-equilibrium radiative heating for Earth aerocapture is demonstrated. It is suggested that two aerobrakes of different sizes will produce optimal-performance for the three phases of the mission (i.e., one aerobrake for Mars aerocapture and descent of the surface lander and another for Earth return).

17. Key Words (Suggested by Author(s))	18. Distribution Statement
Manned Mars mission AOTV Mission analysis	Unclassified-Unlimited Subject Category - 16

19. Security Classif. (of this report)	20. Security Classif. (of this page)	21. No. of pages	22. Price
Unclassified	Unclassified	15	A02